Predictive Speed Control of a Synchronous Permanent Magnet Motor

Esteban J. Fuentes, César Silva
Departamento de Electrónica
Universidad Técnica Federico Santa María
Valparaíso, Chile
Email: cesar.silva@usm.cl

Daniel E. Quevedo, Eduardo I. Silva
ARC Centre for Complex Dynamic Systems and Control
The University of Newcastle
Callaghan, Australia
Email: Daniel.Quevedo@newcastle.edu.au

***Abstract*—This paper presents a predictive strategy for the control of a permanent magnet synchronous motor (PMSM). Our approach allows one to simultaneously manipulate speed and electrical variables, without using any auxiliary linear controller. The high sampling rate, characteristic of this technique, and the limited precision of the typical angle measurement devices, present serious difficulties for this technique to work in practice. These issues are dealt with in the paper and a solution based on an extended Kalman filter is proposed. The effectiveness of the proposed approach is evaluated through simulations.**

I. Introduction

Permanent magnet synchronous motors (PMSM) have high torque and power density, and excellent dynamic characteristics. Thus, they are specially well suited for servo drives and applications where size and weight are major constraints (e.g., automotive and aerospace industry). The typical construction of a PMSM consist of a three phase stator winding and a solid iron rotor with magnets attached to its surface or inserted into the rotor body. This construction results in a magnetic field fixed to the rotor position. Since such machines are not capable of directly starting from the mains, excitation by voltage source inverters controlled by field orientation is required. Control techniques such vector control [1] or direct torque control (DTC) [2] are standard for this type of drives.

The discrete nature of the output voltage in a voltage source inverter, has motivated some authors to use finite alphabet predictive control techniques for current control in this type of power converters [3]. These techniques are also directly applicable to machine drives, and allow one to replace the inner current control loop in vector control, or the inner torque and flux control loops in DTC techniques [4]. Similar approaches have been proposed in, e.g., [5] [6]. Predictive control is a conceptually simple technique based on the prediction of the effects of all possible actuation values on the variables to be controlled, and the subsequent choice of the best actuation value, as measured by an appropriate cost function [3].

It is possible to include different variables into a single cost function. This makes, in principle, possible to achieve integrated multivariable speed and current control. However, some practical implementation issues arise. The main difficulties relate to the large differences between electrical and mechanical dynamics, and also to the quantization noise in the speed measurement which is typical of standard speed sensors in servo drives.

In this paper, we propose solutions for the difficulties mentioned above. We define a cost function designed in a way such that it spectrally shapes some key variables [7], and we use of an extended Kalman filter to smooth the speed feedback signal [8] [9].

The remainder of this paper is organized as follows: the discrete model for the PMSM is developed in Section II and its predictive control is introduced in Section III. In Section IV, the use of a Kalman filter to solve the above mentioned issues is described. In Section V, the proposed speed and current control strategy is tested via simulations. Conclusions are drawn in section VI.

II. The Machine Model

In order to implement a predictive control strategy for a given system, one needs an adequate model for it. This model is used as a predictor of future system states assuming a set of possible actuation values. In this section, we develop a continuous time state space model for a PMSM. This model includes the stator electrical dynamics and the rotor mechanical dynamics. This model is then discretized in order to obtain a model suitable for a discrete time model predictive control formulation (see, e.g., [12]).

A. Continuous Time Machine Model

Using well-known space vector notation [13], the dynamics of the stator of the PMSM can be written as

$$\vec{v}_s = R_s \vec{i}_s + \frac{d\vec{\psi}_s}{dt}, \tag{1}$$

where R_s is the winding resistance, and $\vec{v}_s$, $\vec{i}_s$ and $\vec{\psi}_s$ are the stator voltage vector at the machine terminals, the stator current vector and the vector associated to the flux linked by the stator windings, respectively.

The stator flux linked by the stator windings $\vec{\psi}_s$ has two sources: the field produced by the rotor magnets, which is dependent on the rotor position θ_r, and the self-linked flux due to the current flowing through the stator windings. So, if L_s denotes the stator self-inductance, we have that

$$\vec{\psi}_s = L_s \vec{i}_s + \psi_m e^{j\theta_r}, \tag{2}$$

where ψ_m is the magnitude of the flux due to de rotor magnets. Replacing (2) into (1), the stator dynamics can be written as

$$\vec{v}_s = R_s\vec{i}_s + L_s\frac{d\vec{i}_s}{dt} + j\psi_m\omega_r e^{j\theta_r}, \tag{3}$$

where $\omega_r \triangleq \frac{d\theta_r}{dt}$ is the rotor electrical angular frequency.

Conventional vector control of synchronous machines is usually implemented in a, so-called, dq rotatory frame which is oriented with the rotor magnetic field axis [1]. Using this frame of reference has the advantage of transforming sinusoidal variables into DC values. This yields a model that is similar to that of a DC machine and, hence, to a conceptually simple drive implementation. In this frame, each current component of the synchronous machine has a clear physical meaning: the imaginary component i_{sq} is proportional to the torque, while the real component i_{sd} is proportional to reactive power. Although the implementation of a predictive control strategy could use any reference frame, the synchronous dq frame is preferred in this work for its simple physical interpretation. Transforming the stator dynamics equation into the dq coordinate system results in

$$\vec{v}_s^{(r)} = R_s\vec{i}_s^{(r)} + L_s\frac{d\vec{i}_s^{(r)}}{dt} + j\omega_r\vec{i}_s^{(r)} + j\psi_m\omega_r, \tag{4}$$

where superscript $^{(r)}$ denotes variables in the dq frame, and ω_r is as before. On the other hand, the mechanical rotor dynamics is given by

$$\frac{d\omega_r^m}{dt} = \frac{1}{J}(T_e - T_l) - \frac{B}{J}\omega_r^m, \tag{5}$$

where ω_r^m is the shaft mechanical speed, J is the rotor inertia, T_e is the electric torque produced by the motor, T_l is the load torque[1], and B is a friction coefficient. The rotor speed ω_r^m is directly related to the rotor electrical angular frequency ω_r by the number of pole pairs p of the machine, namely

$$\omega_r = p\,\omega_r^m. \tag{6}$$

The mechanical subsystem (5) is coupled with the stator electrical variables by the electric torque T_e, which, for a non-salient PMSM, is given by

$$T_e = \frac{3}{2}p\,\psi_m i_{sq}. \tag{7}$$

At the same time, the mechanical subsystem interacts with the stator variables through the rotor frequency ω_r, as described in (4). As a consequence, the resulting model is nonlinear (it has a product of two different states). Equations (4), (5), (6) and (7) can be summarized in the following state space representation for the PMSM:

$$\frac{dx(t)}{dt} = g(x(t), u(t)), \tag{8}$$

[1]Which is an independent disturbance and generally unknown.

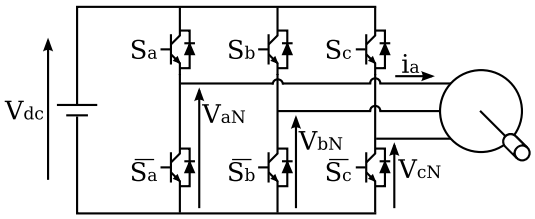

Fig. 1. Two level voltage source inverter

where

$$x \triangleq [i_{sd} \quad i_{sq} \quad \omega_r]^T \tag{9}$$

$$u \triangleq [v_d \quad v_q]^T \tag{10}$$

$$g(x,u) \triangleq \begin{pmatrix} -\frac{1}{\tau_s}i_{sd} + \omega_r i_{sq} + \frac{1}{L_s}v_d \\ -\frac{1}{\tau_s}i_{sq} - \omega_r i_{sd} - \frac{\psi_m}{L_s}\omega_r + \frac{1}{L_s}v_q \\ \frac{pk_T}{J}i_{sq} - \frac{B}{J}\omega_r \end{pmatrix} \tag{11}$$

where $\tau_s \triangleq \frac{L_s}{R_s}$ and $k_T \triangleq \frac{3}{2}p\psi_m$ are the stator time constant and the machine torque constant, respectively.

B. Predictive Model

In order to obtain a predictive model for the motor, the model (8) will be discretized. In order to do so, we use the modified Euler integration method [10]. This yields the following discrete model:

$$\hat{x}[k+1] = x[k] + hg(x[k], u[k]) \tag{12}$$

$$x[k+1] = x[k] + \frac{h}{2}(g(x[k], u[k]) + g(\hat{x}[k+1], u[k])) \tag{13}$$

where h is the sampling interval.

The voltage applied to the motor during each sampling interval belongs to the finite alphabet of actuations generated by the inverter. In this work, a conventional voltage source inverter is considered (see Figure 1). The different output voltage values generated by this converter are determined by the states of the switches in each of its phases, i.e., by S_a, S_b and S_c. Each of these switching functions can adopt values $S_x \in \{0, 1\}$, where $x \in \{a, b, c\}$. The switching state of the inverter can be summarized in a single complex switching function given by

$$\vec{S} \triangleq \frac{2}{3}\left(S_a + \vec{a}S_b + \vec{a}^2 S_c\right), \tag{14}$$

where $\vec{a} \triangleq e^{j2\pi/3}$. This notation allows one to write the output voltage vector $\vec{v}_s$ as

$$\vec{v}_s = V_{dc}\vec{S}, \tag{15}$$

where V_{dc} is the DC-Link voltage (see Fig. 1). Figure 2 shows all possible output voltage vectors.

The output voltage vectors given by (15) are expressed in the stationary frame. In the synchronous dq frame, they become

$$\vec{v}_s^{(r)} = \vec{v}_s e^{-j\theta_r}. \tag{16}$$

Using the seven possible inverter voltage vectors as inputs to the discrete model given by (12) and (13), seven different

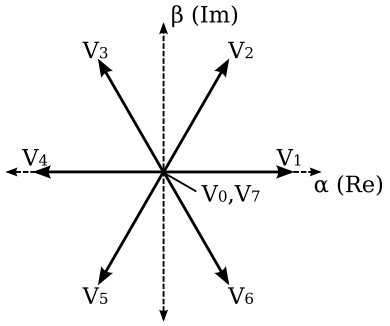

Fig. 2. Voltage vectors generated by the voltage source inverter

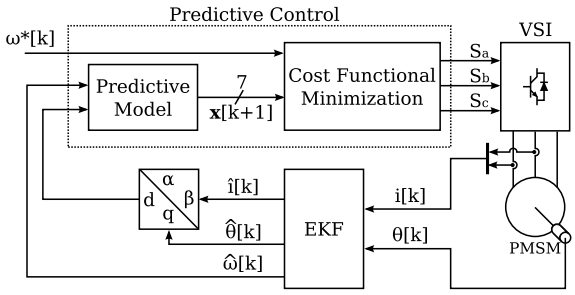

Fig. 3. Predictive Control scheme of the PMSM

predictions for the system state $x = [i_{sd} \quad i_{sq} \quad \omega_r]^T$ are obtained.

Is important to note that, in order to compensate for the algorithm calculation time, the two step prediction scheme proposed in [11] is used. This additional prediction does not change the nature of the control scheme and, hence, to simplify the notation, it will not be considered hereafter.

III. Predictive Control of the PMSM

A diagram of the proposed predictive control scheme is shown in figure 3. In that scheme, the predictive model outputs the seven predicted state vectors of the machine for the next sampling instant. Each of these predictions correspond to one of the possible output voltage vectors the inverter can generate. These predictions are used to evaluate a cost function that weights several control objectives. The voltage vector associated with the predicted state that minimizes the cost function is then selected. This voltage vector is applied to the machine terminals during the next sampling period.

In general, control objectives are multiple, sometimes conflicting, and may be subject to constraints. In the case of speed control for PMSM, the control objectives are as follows:

- Speed reference tracking.
- Smooth behavior of the electrical torque.
- Current magnitude minimization (to achieve good torque per ampere ratios).
- Current limitations (the motor nominal current cannot be exceeded).

These control objectives can be captured by the following cost function:

$$F_c = \lambda_\omega \left(\omega_r^*[k+1] - \omega_r^p[k+1]\right)^2 + \lambda_{id}\left(i_{sd}^p[k+1]\right)^2 + \lambda_{iqf}\left(i_{qf}^p[k+1]\right)^2 + \hat{f}\left(i_{sd}^p[k+1], i_{sq}^p[k+1]\right) \quad (17)$$

where ω_r^* is the speed reference and the superscript $^{(p)}$ denotes predicted values. The symbols and terms in (17) are described next. The first term of the cost function weights the speed error. Its evaluation favors the application of voltage vectors that make the motor speed closest to its reference. For cost functional calculations, the speed reference at the next sampling instant is assumed to be equal to that at the current sampling instant (i.e., $\omega_r^*[k+1] = \omega_r^*[k]$). The second term weights the magnitude of the current in the d axis; its inclusion favors the application of voltage vectors that minimize i_{sd}, i.e., it is aimed at achieving high torque per ampere operation. In the third term, i_{qf}^p is a high-pass filtered version the current in the q axis. This term penalizes the voltage vectors that generate high frequency components in i_{sq}. In this way, a smooth behavior of the electrical torque may be obtained. The first three terms of the cost function are linear functions of the predicted states, and λ_ω, λ_{id} and λ_{iqf} are non-negative weighting factors that give these terms appropriate relative weights, and they can be used for tuning purposes. Although no theoretical rules exist for the design of these weighting factors, some general consideration apply: firstly, the currents factors, λ_{id} and λ_{iqf}, have similar values, reflecting the similar effect that the voltage vectors have in the variation of both currents; secondly, the speed error weighting factor λ_ω must have a relatively high value, in order to compensate for small effect that the voltage vector choice has in the speed variation. The fourth term, i.e., $\hat{f}$, is a highly nonlinear function that takes into account restrictions on the maximum stator current, imposing hard constraints on the maximum values of the stator currents. This function is given by

$$\hat{f}\left(i_{sd}^p, i_{sq}^p\right) \triangleq \begin{cases} \infty & \text{if } |i_{sq}^p| > \hat{i}_q \text{ or } |i_{sd}^p| > \hat{i}_d, \\ 0 & \text{if } |i_{sq}^p| \leq \hat{i}_q \text{ and } |i_{sd}^p| \leq \hat{i}_d. \end{cases} \quad (18)$$

Clearly, $\hat{f}$ penalizes heavily the application of voltage vectors that generate currents beyond acceptable limits. Finally, the voltage vector which minimizes the described cost function is selected and applied to the motor at the beginning of every sampling period. This results in a variable switching frequency, with a theoretical maximum of half the sampling rate.

IV. Implementation Issues

Due to the magnitude of the electrical time constants, the predictive control strategy proposed in the previous section must be implemented at high sampling rates. Otherwise, reasonable current waveforms and smooth torque control cannot be achieved. This leads to considerable noise in the motor speed estimate due to the inherent quantization noise present in the angle output of an incremental encoder. These devices give a quantized measurement of the rotor position, adding high frequency noise to the angle measurement. The quantization

noise in the position measurement is amplified when the speed is estimated using the Euler approximation of the derivative, i.e. when making

$$\tilde{\omega}_r[k] = \frac{\theta_r[k] - \theta_r[k-1]}{h}. \tag{19}$$

It is clear that the noise energy becomes higher when the resolution of the encoder is low or the sampling frequency is increased.

The high magnitude and high frequency noise in the speed estimation produced by the angle quantization, impedes the correct operation of the predictive control strategy proposed above. In this section, we propose a solution to this problem based on the extended Kalman filter (EKF). The EKF is implemented using the usual formulation, given by the following equations [14]:

$$K[k] = P[k|k-1]C^T \left(CP[k|k-1]C^T + R_e\right)^{-1} \tag{20}$$

$$\hat{x}[k|k] = \hat{x}[k|k-1] + K[k]\left(y[k] - C\hat{x}[k|k-1]\right) \tag{21}$$

$$P[k|k] = P[k|k-1] - K[k]CP[k|k-1] \tag{22}$$

$$\hat{x}[k+1|k] = g_d(\hat{x}[k|k], u[k]) \tag{23}$$

$$P[k+1|k] = A[k]P[k|k]A[k]^T, \tag{24}$$

where $\hat{x}$ is the state estimate, $g_d(x,u)$ is the discrete model of the nonlinear system, A is the corresponding jacobian matrix, and C is the model output matrix. R_e and P are the covariance matrices of the measurement noise and the state, respectively, and K is the Kalman gain. In (23) and (24) the state and its covariance are predicted using the measurements available at the sampling instant k. These predictions are then corrected with new data at the next sampling instant by (21) and (22) using the Kalman gain calculated in (20).

To implement the EKF, the stationary frame machine model, i.e. $\alpha\beta$ frame model, is preferred because, when doing so, the quantization noise in the angle measurement is not propagated into the electrical variables through a coordinate rotation. Additionally, in the stationary frame, the rotor speed has a grater effect in the electrical dynamics and, hence, the current measurements have a bigger influence in the estimation of the mechanical variables, as compared with an implementation the dq rotatory frame.

The continuous model of the machine in the $\alpha\beta$ frame is given by the following equations:

$$\frac{dx_{\alpha\beta}(t)}{dt} = g_{\alpha\beta}(x_{\alpha\beta}(t), u_{\alpha\beta}(t)) \tag{25}$$

$$y_{\alpha\beta}(t) \triangleq [i_\alpha \quad i_\beta \quad \theta_r]^T = Cx_{\alpha\beta}(t), \tag{26}$$

where

$$x_{\alpha\beta} \triangleq [i_\alpha \quad i_\beta \quad \omega_r \quad \theta_r]^T \tag{27}$$

$$u_{\alpha\beta} \triangleq [v_\alpha \quad v_\beta]^T \tag{28}$$

$$C_{\alpha\beta} \triangleq \begin{bmatrix} 1 & 0 & 0 & 0 \\ 0 & 1 & 0 & 0 \\ 0 & 0 & 0 & 1 \end{bmatrix} \tag{29}$$

$$g_{\alpha\beta}(x,u) \triangleq \begin{pmatrix} -\frac{1}{\tau_s} i_\alpha + \frac{\psi_m}{L_s}\omega_r \sin(\theta_r) + \frac{1}{L_s} v_\alpha \\ -\frac{1}{\tau_s} i_\beta - \frac{\psi_m}{L_s}\omega_r \cos(\theta_r) + \frac{1}{L_s} v_\beta \\ \frac{pk_T}{J}(-\sin(\theta_r) i_\alpha + \cos(\theta_r)) - \frac{B}{J}\omega_r \\ \omega_r \end{pmatrix}. \tag{30}$$

Note that $y_{\alpha\beta}$ corresponds to the state variables that are available for measurement. The third state, namely ω_r, is not measured, but estimated using the EKF.

The model in (25) is discretized for the implementation of the EKF using the modified Euler integration method mentioned earlier.

The EKF tuning is made adjusting the initial covariance matrix $P[0,-1]$ and the measurement noise covariance matrix R_e. For simplicity, we assume R_e to be diagonal. The entry associated with the rotor angle measurement corresponds to the quantization noise variance σ_q^2. Assuming uniform and white quantization noise,

$$\sigma_q^2 = \frac{\Delta^2}{12}, \tag{31}$$

where Δ is the quantization step (i.e., is given by the encoder resolution). The remaining entries in the R_e matrix, are associated with the currents measurements (i_α, i_β), and were adjusted empirically through simulations.

Another drawback of employing a high sampling rate is the magnification of the effect of the commutation dead-time of the semiconductors. In these conditions, it cannot be disregarded. This is particularly true for the EKF, whose performance is heavily affected if the dead times are not taken into account.

The commutation dead-time corresponds to a delay on the turn-on of the semiconductors. This gives time for the corresponding complementary switch to completely turn-off, thus avoiding short circuits of the DC link during commutation. This delay on the turn-on of the switches has an effect on the output voltage, reducing or increasing its average value with respect to its reference depending on the commutation state and current direction. This effect on the inverter output voltage is depicted in Figure 4.

Dead-time effects can be taken into account in the input voltages of the EKF by correcting the reference voltage according to the measured phase current. We propose the following:

$$V_{zN}[k] = V_{zN}^*[k] + V_{zDT}[k], \tag{32}$$

where V_{zN}^* is the reference voltage for a given phase $z \in \{a,b,c\}$, and V_{zDT} is the dead-time compensation voltage for

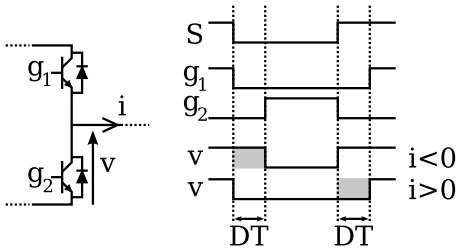

Fig. 4. Effect of the commutation dead-time of the semiconductors on the inverter output voltage

that phase, which is given by

$$V_{zDT}[k] = \begin{cases} 0 & \text{if } S_z[k] = S_z[k-1] \\ -\frac{\mathrm{DT}}{h} V_{dc} & \text{if } S_z[k] - S_z[k-1] = -1 \\ & \quad \text{and } i_z > 0 \\ \frac{\mathrm{DT}}{h} V_{dc} & \text{if } S_z[k] - S_z[k-1] = 1 \\ & \quad \text{and } i_z < 0, \end{cases} \tag{33}$$

where DT corresponds, approximately, to the dead-time value and its magnitude can be adjusted to include compensation of other related effects, such as device commutation time and conduction voltage drop [15].

Using the reference voltage (appropriately corrected for the dead-time), and the currents and rotor position measurements as inputs to the EKF, a good estimation of the rotor speed is achieved. This speed estimate has no high frequency quantization noise, and can be used as speed measurement in the proposed predictive control strategy.

V. Simulation Results

The proposed predictive control strategy is evaluated through simulations using MATLAB/Simulink. The parameters of a real $4[kW]$ machine were used in this simulation and they are listed in Table I. The simulated inverter is characterized by a DC link of $540[V]$ and dead-time of $2[\mu s]$.

For the purposes of prediction and evaluation of the objective function, a sampling period $h = 30[\mu s]$ was used. In each sampling period, predictions were performed using the prediction model described in (12) and (13) for all voltage vectors shown in Figure 2. The results of these predictions were then used to evaluate the cost function (17), which has the parameters shown in Table II. The high-pass filter for i_{sq} was a second order butterworth filter with cutoff frequency f_c. This predictive model, and the evaluation of the cost function, was coded as a Matlab S-function in the C language for easy migration to an experimental set-up. The machine, on the other hand, was simulated using continuous time Simulink integrators and a sampling frequency much higher than h^{-1}.

Steady state results are shown in Figure 5. This result assumes additional friction as mechanical load. The effect of using an EKF is evident, showing a significant improvement on the estimated speed $\hat{\omega}_r$, with respect to the speed calculated using the Euler approximation $\tilde{\omega}_r$. For this speed calculation, an angle measurement with a resolution of 4096 [PPR] and a sampling period of $30[\mu s]$ has been used. Also, the stator currents show low harmonic distortion, which is a consequence of imposing zero reference for i_{sd}.

TABLE I
Machine Parameters.

Parameter	Value
R_s	$0.3[\Omega]$
L_s	$8.2[mH]$
ψ_m	$0.125[Wb]$
p	3
J	$0.004[kgm^2]$
B	$1 \cdot 10^{-3}[kgm^2/s]$

TABLE II
Predictive Control Parameters

Parameter	Value
h	$30[\mu s]$
λ_ω	1000
λ_{id}	1
λ_{iqf}	1.4
f_c	$200[Hz]$
$\widehat{i}_q$	$22.6[A]$
$\widehat{i}_d$	$1[A]$

The transient response, under the same conditions, is shown in Figure 6, where a speed reversal is documented. The first noticeable characteristic of this response is its good reference speed tracking, and a fast response in the torque current i_{sq}. Remarkable is the fact that the speed shows almost no overshoot, while the torque transient (proportional to i_{sq}) is adjusted to obtain nearly ideal speed tracking. We also note that the control of the current components i_{sd} and i_{sq} is highly decoupled, achieving almost zero i_{sd} current. As mentioned above, this leads to highly sinusoidal stator currents, even during transients. Finally, some oscillations are noticeable on the control of i_{sq} at the beginning of the simulation. This is due to the transient response of the EKF, which translates into a speed estimation error at start-up. This error converges to zero in less than $0.04[s]$.

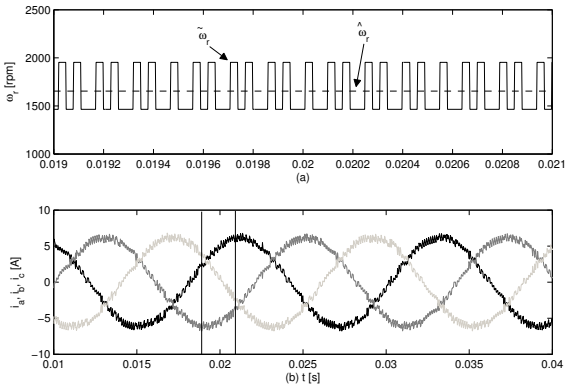

Fig. 5. Steady state operation: (a) rotor speed calculated using the Euler approximation $\tilde{\omega}_r$ and the Kalman filter $\hat{\omega}_r$, (b) stator currents.

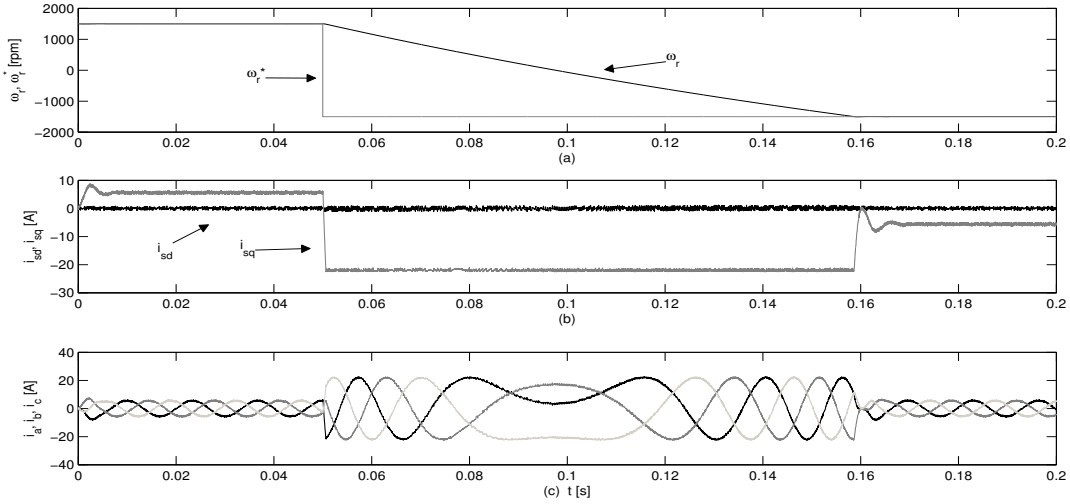

Fig. 6. Speed reversal: (a) reference and actual rotor speed, (b) stator currents in dq frame, (c) three-phase stator currents.

VI. Conclusions

In this paper, we have developed a centralized predictive control strategy for a PMSM. A suitable cost function that incorporates different control objectives, including constraints, has been designed. The proposed cost function is more complex than a simple weighted sum of errors in the different objectives, including filters and nonlinear functions for a smooth torque response. On the other hand, the inclusion of restrictions was straightforward once a suitable nonlinear term was included in the cost function. The resulting scheme showed good performance, which is characterized by good speed tracking and decoupled current control.

The high sampling rate needed for effective current control using the proposed predictive control leads to serious implementation difficulties. This is particularly true in relation to quantization noise in the speed feedback signal. An extended Kalman filter has been designed to solve this problem. Nevertheless, this filter complicates the control strategy. We conclude that measurement noise may become a serious issue in high speed predictive control, but an appropriately designed Kalman filter can be used to mitigate such problems.

Finally, it should be noted that there exists hard constraints on the sampling frequency due to physical limitations such as A/D conversion time, maximum allowable switching frequency on the semiconductors and DSP calculation time which, in a real implementation, might be high due to the complexity of the motor model and the addition of the Kalman filter. On the other hand, the low inductance characteristic of PMSM motors impose restrictions on the minimum sampling frequency needed to achieve good current control. A good trade-off may not be achieved if the inductance of the machine is too small.

Experimental validation of the proposed control scheme is ongoing.

References

[1] T. Jahns, G. Kliman, T. Neumann, "Interior Permanent-Magnet Synchronous Motors for Adjustable-Speed Drives," *IEEE Trans. Ind. Appl.*, vol. IA-22, pp. 748–747, 1986.

[2] L. Tang, L. Zhong, M.F. Rahman, Y. Hu, "A novel direct torque control for interior permanent-magnet synchronous machine drive with low ripple in torque and flux - a speed-sensorless approach," *IEEE Trans. Ind. Appl.*, vol. 39, pp. 1748–1756, 2003.

[3] J. Rodríguez, J. Pontt, C. Silva, P. Correa, P. Lezana, P. Cortés, U. Hammann, "Predictive Current Control of a Voltage Source Inverter," *IEEE Trans. Ind. Electron.*, vol. 54, pp. 495–503, 2007.

[4] F. Morel, J. M. Retif, X. Lin-Shi, B. Allard, P. Bevilacqua, "A Predictive Control for a Matrix Converter-Fed Permanent Magnet Synchronous Machine," *in Proc. 39th IEEE PESC*, Rhodes, Greece, pp. 15–21, 2008.

[5] H. Le-Huy, K. Slimani, P. Viarouge, "Analysis and Implementation of a Real-Time Predictive Current Controller for Permanent-Magnet Synchronous Servo Drives," *IEEE Trans. Ind. Electron.*, vol. 41, pp. 110–117, 1994.

[6] M. Pacas, J. Weber, "Predictive Direct Torque Control for the PM Synchronous Machine," *IEEE Trans. Ind. Electron.*, vol. 52, pp. 1350–1356, 2005.

[7] P. Cortés, J. Rodríguez, D. E. Quevedo, C. Silva, "Predictive Current Control Strategy With Imposed Load Current Spectrum," *IEEE Trans. Power Electron.*, vol. 23, pp. 612–618, 2008.

[8] Z. Xu, M. F. Rahman, "An Extended Kalman Filter Observer for the Direct Torque Controlled Interior Permanent Magnet Synchronous Motor Drive," *in Proc. PEDS.*, pp. 686–691, 2003.

[9] R. Dhaouadi, N. Mohan, L. Norum, "Design and Implementation of an Extended Kalman Filter for the State Estimation of a Permanent Magnet Synchronous Motor," *IEEE Trans. Power Electron.*, vol. 6, pp. 491–497, 2008.

[10] R. Burden, J. Faires, A. Reynolds, *Numerical Analysis,* Prindle, Weber & Schmidt, Boston, Mass., 1978.

[11] P. Cortés, J. Rodríguez, D. E. Quevedo, C. Silva, "Predictive Current Control Strategy With Imposed Load Current Spectrum," *IEEE Trans. Power Electron.*, vol. 23, pp. 612–618, 2008.

[12] E. Camacho, C. Bordons, *Model Predictive Control,* Springer, 2004.

[13] W. Leonhard, *Control of Electrical Drives,* Springer, 1997.

[14] S. Bolognani, L. Tubiana, M. Zigliotto, "Extended Kalman Filter Tuning in Sensorless PMSM Drives," *IEEE Trans. Ind. Appl.*, vol. 39, pp. 1741–1747, 2003.

[15] J.-W. Choi, S.-K. Sul, "Inverter Output Voltage Synthesis Using Novel Dead Time Compensation," *IEEE Trans. Power Electron.*, vol. 11, pp. 221–227, 1996.